Taylor & Francis
Taylor & Francis Group

Journal of Enzyme Inhibition and Medicinal Chemistry

ISSN: 1475-6366 (Print) 1475-6374 (Online) Journal homepage: https://www.tandfonline.com/loi/ienz20

An evolutionarily conserved allosteric site modulates beta-lactamase activity

Fatma Gizem Avci, Fatma Ece Altinisik, Didem Vardar Ulu, Elif Ozkirimli Olmez & Berna Sariyar Akbulut

To cite this article: Fatma Gizem Avci, Fatma Ece Altinisik, Didem Vardar Ulu, Elif Ozkirimli Olmez & Berna Sariyar Akbulut (2016) An evolutionarily conserved allosteric site modulates beta-lactamase activity, Journal of Enzyme Inhibition and Medicinal Chemistry, 31:sup3, 33-40, DOI: 10.1080/14756366.2016.1201813

To link to this article: https://doi.org/10.1080/14756366.2016.1201813

Journal of Enzyme Inhibition and Medicinal Chemistry

www.tandfonline.com/ienz
ISSN: 1475-6366 (print), 1475-6374 (electronic)

J Enzyme Inhib Med Chem, 2016; 31(S3): 33–40
 DOI: 10.1080/14756366.2016.1201813

Taylor & Francis
Taylor & Francis Group

RESEARCH ARTICLE

An evolutionarily conserved allosteric site modulates beta-lactamase activity

Fatma Gizem Avci[1], Fatma Ece Altinisik[1], Didem Vardar Ulu[2], Elif Ozkirimli Olmez[3], and Berna Sariyar Akbulut[1]

[1]Department of Bioengineering, Marmara University, İstanbul, Turkey, [2]Department of Chemistry, Boston University, Boston, MA, USA, and [3]Department of Chemical Engineering, Bogazici University, İstanbul, Turkey

Abstract

Declining efficiency of antibiotic-inhibitor combinatorial therapies in treating beta-lactamase mediated resistance necessitates novel inhibitor development. Allosteric inhibition offers an alternative to conventional drugs that target the conserved active site. Here, we show that the evolutionarily conserved PWP triad located at the N-terminus of the H10 helix directly interacts with the allosteric site in TEM-1 beta-lactamase and regulates its activity. While point mutations in the PWP triad preserve the overall secondary structures around the allosteric site, they result in a more open and dynamic global structure with decreased chemical stability and increased aggregation propensity. These mutant enzymes with a less compact hydrophobic core around the allosteric site displayed significant activity loss. Detailed sequence and structure conservation analyses revealed that the PWP triad is an evolutionarily conserved motif unique to class A beta-lactamases aligning its allosteric site and hence is an effective potential target for enzyme regulation and selective drug design.

Keywords

Allostery, class A beta-lactamases, inhibition, PWP conservation, structure function relationship, TEM-1

History

Received 17 March 2016
Revised 1 June 2016
Accepted 6 June 2016
Published online 29 June 2016

Introduction

Beta-lactamases are ancient enzymes that have been synthesized as a response to the action of beta-lactam antibiotics. With the pressure arising from the irresponsible misuse of beta-lactam antibiotics, these enzymes continue to evolve to increase enzyme fitness. This evolutionary persistence of beta-lactamase enzymes makes antibiotic resistance a global health threat[1–6]. Currently, there is a vast variety of beta-lactamase inhibitors[7] that are co-administered with antibiotics to enhance drug efficacy. Unfortunately, many of the over 1300 different beta-lactamases can rapidly hydrolyze these inhibitors rendering them ineffective. In this context, continued search for novel inhibitors is an area of intense research[8,9].

Beta-lactamases are classified into four classes (A, B, C and D) based on sequence similarity[10,11]. Although they all share a common fold, their active site characteristics differ sufficiently to allow for recognition of different ligands and different catalytic mechanisms. Classes A, C and D are all serine hydrolases, while class B beta-lactamases are zinc binding enzymes. Classification based on ligand recognition is consistent with the Ambler classification but shows that the active site of class A and C beta-lactamases recognizes similar ligands while class B and D beta-lactamases each have their own specific ligands different from classes A and C[7,11,12].

Class A beta-lactamases are the most prevalent class in hospital infections. Members belonging to this class have a common fold with a very well conserved active site. Current class A beta-lactamase inhibitors in use, all target this active site. TEM-1 beta-lactamase, which is the most extensively studied member of this class, has been examined using mutagenesis[13], X-ray crystallography[14], NMR spectroscopy[15] and molecular dynamics (MD) simulations[16]. It has sequence identities ranging from 53 to 79% in pairwise alignments with the ancestral forms of beta-lactamase and share the conserved beta-lactamase fold[17].

Allosteric inhibition is an attractive alternative for drug design studies because allosteric inhibitors are more selective than drugs that target the active site, which is conserved across the enzyme family[16,18,19]. The presence of an allosteric binding site for TEM-1 was first recognized by Horn and Shoichet (2004) who showed that the H10 helix moves away from the protein core to allow binding of allosteric inhibitors to a hydrophobic pocket formed by the two helices, H10 and H11 on one side and the β-sheet composed of β3, β4, β5 on the other. This binding site is located about 16 Å away from the active site serine, S70, of TEM-1 beta-lactamase[18]. The H10 helix C-terminus forms part of the active site, specifically K243 participating in catalysis and substrate binding, while P226–W229–P252 (PWP triad) residues at the N-terminus participate in aromatic ring stacking that stabilize the helix. Together with the T-shaped aromatic interaction between W229 and W290[14], this extensive interaction network modulates the flexibility of H10 and its interactions with other secondary structural elements in the hydrophobic inhibitor binding pocket, suggesting the contribution of these residues to allostery[16]. Interestingly, the crystallization adjuvant CYMAL-6 binds to this hydrophobic pocket in the crystal structure of SHV-1, which is another class A beta-lactamase[20]. Binding of CYMAL-6 to the ridge between the H10 and H11 helices of SHV-1 resulted in

Address for correspondence: Berna Sariyar Akbulut, Bioengineering Department, Marmara University, 34722 Kadikoy, Istanbul, Turkey. Tel: +90 216 348 0292 ext. 1721. Fax: +90 216 345 0126. E-mail: berna.akbulut@marmara.edu.tr

approximately 20% reduction in reaction velocity[21]. Similarly, MD simulations and free energy calculations performed with wild type and W229A mutant forms of TEM-1 and SHV-1 beta-lactamases showed that beta-lactamase inhibitor protein (BLIP) binding to the active site was less favorable for the mutant, possibly due to loss of the PWP triad stacking interaction[16]. The binding of the allosteric inhibitors to the hydrophobic cavity between H10 and H11 and the β-sheet formed by β3-β4-β5, as well as the MD simulation results suggest that the relative orientation of H10 with respect to the β-sheet and its flexibility are critical for beta-lactamase activity. Even a slight disruption to the structural integrity around H10 may be amplified through the secondary structural elements, resulting in a significant impact on the allosteric site in the hydrophobic core.

To assess the significance of the PWP triad for enzyme activity and allosteric regulation, we created point mutations within the PWP triad and performed functional assays and structural characterizations to study the impact of these mutations on enzyme structure and activity. We also examined the conservation of these residues within the primary, secondary and tertiary structures of the beta-lactamases using structural bioinformatics to evaluate the significance and generalizability of our findings.

Materials and methods

Cloning of *bla*$_{TEM-1}$ gene, mutagenesis and transformation

The designed forward (Fwd) and reverse (Rev) *bla* primers given in Table 1 were used to amplify the *bla*$_{TEM-1}$ gene of pUC18 (our laboratory stock) using polymerase chain reaction with the following conditions: initial denaturation at 95 °C for 3 min, followed by 35 cycles of denaturation at 95 °C for 1 min, annealing at 56 °C for 1 min, extension at 72 °C for 2 min and a final extension for 10 min at 72 °C. The amplified gene was digested with *Xho*I and *Nco*I enzymes (Fermentas, Waltham, MA) and ligated into the corresponding sites in the pET28a(+) cloning vector (our laboratory stock). The resulting gene product contained a C-terminal 6xHis tag. The presence of *bla*$_{TEM-1}$ gene in the recombinant plasmid, pET-FGA*bla*, was verified by sequencing.

The point mutations W229A, W229F, W229Y, P226A and P252A were introduced into the *bla*$_{TEM-1}$ gene cloned in pET28a(+) using QuikChange Site Directed Mutagenesis Kit (Agilent Technologies, Santa Clara, CA) following the manufacturer's protocol. The designed primers were purchased from Integrated DNA Technologies (IDT, Coralville, IA). Primers used for mutagenesis are listed in Table 1. Sequences of constructed mutant plasmids were verified by DNA sequencing.

All the constructed plasmids were transformed using $CaCl_2$ method into *Escherichia coli* XL1 cells (our laboratory stock) for archiving and into *E. coli* BL21 (DE3) cells (TUBITAK-GEBI) for expression[22].

TEM-1 beta-lactamase expression and purification

E. coli BL21 (DE3) cells with any of the *bla*$_{TEM-1}$ carrying plasmids were grown in Luria Bertani (LB) medium supplemented with 50 μg mL^{-1} kanamycin. Precultures were prepared overnight at 37 °C and 180 rpm and 1 mL of preculture was used to inoculate 100 mL of fresh LB. Protein expression was induced with 0.1 mM isopropyl β-D-1-thiogalactopyranoside when OD_{600} of cells reached 0.8 and cells were allowed to grow for 5 h at 30 °C and 180 rpm. Cells were harvested and periplasmic proteins were extracted using osmotic shock procedure[23]. TEM-1 beta-lactamase in the crude extract was purified by Ni^{2+}-affinity chromatography using HisLink™ Protein Purification Resin (Promega, Fitchburg, WI). Beta-lactamase containing fractions were eluted using a buffer of 50 mM NaH_2PO_4 and 300 mM NaCl with 250 mM imidazole (pH 8.0). Protein concentration was measured with the method of Bradford[24]. Purity of the protein samples was verified by electrophoretic analysis.

Refolding with urea

After extraction of periplasmic proteins, remaining pellets were resuspended in 5 mL 50 mM Tris buffer (pH 7.8). The samples were disrupted by sonication on ice. Cytoplasmic extracts containing intracellular proteins were removed and the remaining cell pellet was resuspended in 10 mL 8M urea solution to dissolve protein aggregates. Solubilized protein aggregates were electrophoretically analyzed on SDS polyacrylamide gels.

Measurement of beta-lactamase activity

Beta-lactamase was assayed by monitoring the hydrolysis of its substrate CENTA (Calbiochem, San Francisco, CA) at 405 nm as described previously[8]. The reaction was carried out at 25 °C in a total volume of 1 mL in 50 mM K^+PO_4 buffer (pH 7.0) with 47 μM CENTA. One Unit (U) of beta-lactamase activity was defined as the amount of enzyme that hydrolyzed 1 μmol of CENTA per minute at 25 °C.

Electrophoretic analysis of proteins and zymogram

Both SDS polyacrylamide gel electrophoresis (PAGE) and native PAGE were used to analyze periplasmic proteins. Native PAGE was carried out using the standard SDS-PAGE protocol[25], but without SDS in the gels and the samples. Gels were stained with Coomassie Brilliant Blue G-250 dye to visualize the proteins[26]. For the zymograms, native gels were equilibrated in 50 mM potassium phosphate buffer (pH 7.0) at room temperature for 45 min (3×15 min). Beta-lactamase activity was visualized by the appearance of yellow bands after overlaying the gel with 50 mM K^+PO_4 buffer (pH 7.0) containing 47 μM CENTA.

Table 1. Primers used in this study.

Name		Sequence
bla	Fwd	5′ CGA CCA TGG ATG AGT ATT CAA CAT TTC CG 3′
	Rev	5′ CAG TGA AGC CTC GAG CCA ATG CTT AAT 3′
W229A	Fwd	5′ CG GCC CTT CCG GCT GGC GCG TTT ATT GCT GAT AAA TCT GG 3′
	Rev	5′ CC AGA TTT ATC AGC AAT AAA CGC GCC AGC CGG AAG GGC CG 3′
W229F	Fwd	5′CG GCC CTT CCG GCT GGC TTC TTT ATT GCT GAT AAA TCT GG 3′
	Rev	5′ CC AGA TTT ATC AGC AAT AAA GAA GCC AGC CGG AAG GGC CG 3′
W229Y	Fwd	5′ CG GCC CTT CCG GCT GGC TAC TTT ATT GCT GAT AAA TCT GG 3′
	Rev	5′ CC AGA TTT ATC AGC AAT AAA GTA GCC AGC CGG AAG GGC CG 3′
P226A	Fwd	5′ CTG CGC TCG GCC CTT GCG GCT GGC TGG TTT ATT GC 3′
	Rev	5′ GC AAT AAA CCA GCC AGC CGC AAG GGC CGA GCG CAG 3′
P252A	Fwd	5′ C ATT GCA GCA CTG GGG GCA GAT GGT AAG CCC TCC 3′
	Rev	5′ GGA GGG CTT ACC ATC TGC CCC CAG TGC TGC AAT G 3′

Sample preparation for structural studies

Wild-type and mutant beta-lactamase enzymes were exhaustively dialyzed against 20 mM Na_2HPO_4 buffer (pH 7.0) to remove imidazole and NaCl and were spin filtered to prepare the samples used for structural studies. A single 350 µL of protein sample was prepared and used for each enzyme construct to perform circular dichroism, fluorescence spectroscopy and size exclusion chromatography (SEC). Protein concentration was determined by ultraviolet-visible absorbance at 280 nm using an extinction coefficient of 28 085 M^{-1} cm^{-1} for constructs retaining W229 and 22 585 M^{-1} cm^{-1} for constructs with W229 point mutations, as well as SDS-PAGE gel band quantification.

Circular dichroism

Far-UV CD spectra were acquired in a 2 mm cuvette from 185 to 250 nm with 1 nm steps using a 1 nm bandwidth, and 10 s averaging time, at 20 °C, on an AVIV 62 DS CD Spectrometer equipped with Peltier temperature controller (Boston University Medical Center, Department of Physiology and Biophysics). The thermal melts were performed at 222 nm from 5 °C to 80 °C in 1 °C steps, with a 30 s averaging time for each temperature step.

Tryptophan fluorescence

For each enzyme construct, the sample was excited at 295 nm using a 5 mm slit width. The corresponding fluorescence emission was recorded from 300 to 450 nm in 0.5 nm increments at 20 °C on a Varian Cary Eclipse (Boston University Medical Center, Department of Physiology and Biophysics).

Size exclusion chromatography

After completion of the CD and fluorescence experiments, the samples were applied onto a Superdex-75 analytical column (GE Healthcare, Little Chalfont, UK) in 20 mM sodium phosphate buffer, pH 7.5 and 150 mM NaCl running buffer at a flow rate of 0.5 mL min^{-1} using the Bio-Rad Dual Chromatography system (Wellesley College, Department of Chemistry).

Sequence and structure conservation

The conservation of W229, P226, P252 and W290 was examined using the Consurf server[27,28]. TEM-1 beta-lactamase crystal structure (PDB ID: 1ZG4) was used to obtain homologs using CS-Blast with maximal 95% and minimal 35% ID between sequences for homology. The homologs were collected from UNIREF90. The sequences were aligned using MAFFT and the conservation score of each residue was calculated using Bayesian algorithm. Residues with high conservation received a score of 9, while those with low conservation received a score of 1. To check the structural conservation of the PWP stacking interaction, swisspdb[29] was used to search for the PWP motif in the 90% nonredundant set of 14 341 X-ray structures. Structural features around the PWP triad were examined for a representative set of beta-lactamases.

Results and discussion

Point mutations of the tryptophan residue in the PWP triad cause subtle structural changes that alter enzyme activity significantly

To assess the individual contributions of the residues within the PWP triad to the structural integrity and activity of the enzyme, two sets of point mutants were studied. The first set consisted of alanine mutants of the three residues in the triad P226A, W229A and P252A and these mutants were used to determine the relative importance of each member of the triad to enzyme activity. The second set consisted of aromatic point mutants of the tryptophan residue in the triad, W229F and W229Y, and were used in conjunction with W229A to gain additional insight into the impact of amino acid size, aromaticity, and polarity for the structurally and functionally important interactions within class A beta-lactamases.

Zymograms of the native gels for W229F and W229Y mutant enzymes possessed partial activity, as indicated by the darker regions on the gel resulting from CENTA hydrolysis, while the W299A mutant lacked activity (Figure 1A and B). These bands corresponded to beta-lactamase bearing regions on the native gels. However, enzymatic activities of the purified enzymes, also measured using CENTA as the substrate, showed a significant loss in the beta-lactamase activity for all three W229 mutants (Table 2). Tryptophan is the largest amino acid occupying a volume of 240 $Å^3$. Substitution of tryptophan with tyrosine and phenylanaline (each occupying a volume of 203 $Å^3$) is expected to result in a significant decrease in van der Waals interactions or a significant molecular rearrangement to reoptimize these interactions around this side chain without impacting aromaticity. Comparing the amount of activity between wild-type and the W229F or W229Y mutants reveals that both substitutions result in a similar and significant loss of activity indicating that the size but not the polarity of the side chain has an important effect on enzyme activity. Removal of the aromatic side chain from this position, as reflected by the W229A mutant, resulted in an almost complete activity loss, underscoring the significance of size and possibly the aromaticity of the side chain at this position. Hence activity measurements were consistent with the zymogram analysis. Overall, this finding highlights the absolute conservation of the tryptophan residue at this location to ensure optimal arrangement of the structural elements extending into the active site through the hydrophobic pocket of the allosteric region.

Similar activity assays performed on enzymes harboring point mutations flanking the central tryptophan residue in the PWP triad (P226A and P252A) also showed about five- to 10-fold loss in enzyme activity (Figure 2A and B, Table 2). These results clearly demonstrate that the integrity of the entire stacking interaction network established by the PWP triad is essential for optimized enzyme activity.

Analysis of purified enzymes harboring a mutation at W229 on native electrophoretic gels indicates slight differences in the migration profile of each mutant compared to the wild-type, as well as to each other. The mutant forms travelled close to their monomeric molecular weights, however exhibited a more diffuse and slower migration than the wild-type (Figure 1A). We observed similar alterations in the migration profiles of also the proline point mutants on native electrophoretic gels (Figure 2A).

Analytical SEC data for the three W229 mutants confirmed an increase in the apparent molecular weight of the mutant enzymes indicating a slightly larger hydrodynamic radius compared to the wild type. SEC data also revealed diminished chemical stability in the mutants, as evidenced by the presence of multiple proteolysis products that were absent from the wild-type sample, as well as significant increase in the aggregation propensity for the mutants (data not shown). Taken together, these results suggest a more open and dynamic global structure with decreased chemical stability and increased aggregation propensity for the mutants compared to a more tightly packed, chemically stable and soluble wild-type enzyme.

To investigate if the point mutations at W229 resulted in any major unfolding of the secondary structures in TEM-1, we performed CD experiments on the wild-type and as on the three W229 mutants, W229A, W229F and W229Y. During sample

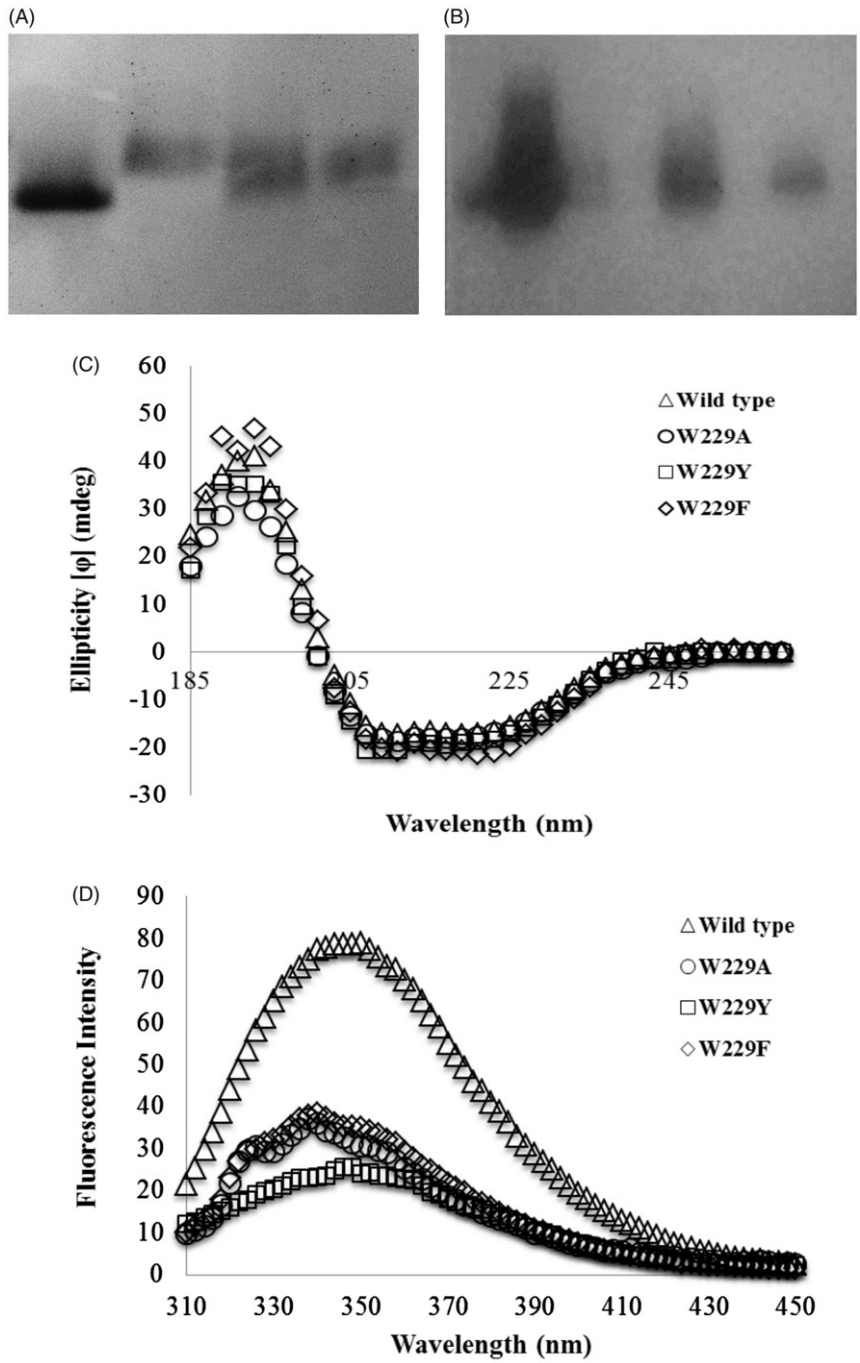

Figure 1. Analysis of purified W229 beta-lactamase mutants (W229A, W229F and W229Y) and wild-type beta-lactamase; (A) native gel stained with Coomassie Brilliant Blue G-250, (B) zymogram of the native gel and (C) far-UV CD spectra of the beta-lactamase constructs. The ellipticity data for the mutant samples were adjusted for concentration to be equivalent to the concentration of wild-type (~5 μM). The spectra were acquired in a 2 mm cuvette from 185 to 250 nm with 1 nm steps using a 1 nm bandwidth, and 10 s averaging time, at 20 °C, on an AVIV 62 DS CD spectrometer equipped with Peltier temperature controller, and (D) fluorescence emission spectra of the beta-lactamase constructs. The samples were excited at 295 nm and the emission was recorded from 300 to 450 nm in 0.5 nm increments at 20 °C. To allow for direct comparison of the fluorescence emission data, the fluorescence intensity for the mutant samples were normalized to wild-type to reflect equimolar (~5 μM) concentrations.

Table 2. Activity of wild-type and mutant beta-lactamases.

	% Relative activity
Wild-type	100 ± 13.8
W229A	2 ± 0.6
W229Y	16 ± 2.3
W229F	18 ± 3.4
P226A	8 ± 2.4
P252A	15 ± 3.1

preparation, it was observed that all mutant enzymes displayed a significant decrease in solubility and were much more prone to aggregation. However, the data collected on dilute, soluble enzyme samples displayed CD spectra that were virtually superimposable on that of wild-type after appropriate concentration correction, indicating no significant change in the secondary structure of the enzyme between the wild-type and the mutants (Figure 1C).

The thermal melt experiments performed on the wild-type enzyme and the three W229 point mutants showed that for the first major unfolding of the enzyme, the T_m was around 48 °C occurring over a temperature range of ~23 °C (35–58 °C) for both the wild-type and the three W229 mutants, indicating that there is not a significant loss in thermal stability for the point mutants compared to the wild-type enzyme.

Tryptophan is a dominant intrinsic fluorophore in proteins and its emission maximum is highly dependent upon polarity and/or local environment. In a completely apolar environment, tryptophan displays a characteristic blue-shifted structured emission, whereas a tryptophan residue exposed to water or one with an

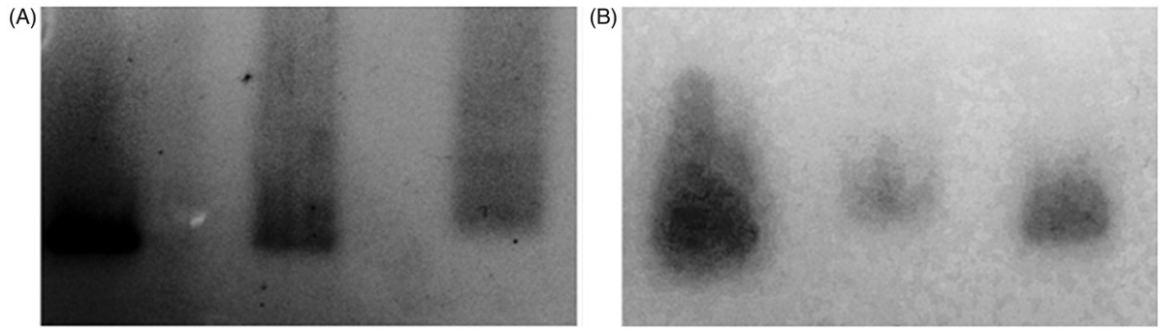

Figure 2. Analysis of purified P252A and P226A beta-lactamase mutants and wild-type beta-lactamase; (A) native gel stained with Coomassie Brilliant Blue G-250 and (B) zymogram of the native gel.

indole ring engaged in specific H-bonds, displays an emission shifted to longer wavelengths. A protein that contains multiple tryptophan residues is expected to display an emission spectrum that reflects the average environment of all the tryptophan residues, but their contributions may be unequal. TEM-1 beta-lactamase contains four tryptophan residues (W165, W210, W229 and W290). Based on the crystal structure of TEM-1, W229 and W290 are in close proximity within the alpha/beta domain housing the allosteric site, while W165 and W220 are located on the other all-alpha domain of the enzyme. Solvent accessibility analysis for these four tryptophan residues using the program DSSP indicated that two of these residues W210 and W229 are highly solvent inaccessible while W165 and W290 are relatively solvent accessible. In addition, analysis of the TEM-1 crystal structure, which contains bound water molecules, indicates that W210 and W290 are engaged in H-bonds to neighboring water molecules. Therefore, W210 and W229 are expected to display a more blue-shifted emission compared to W210 and W290.

TEM-1 also contains four tyrosine residues that can potentially contribute to the emission spectrum during fluorescence experiments. To avoid the excitation of the four tyrosine residues and to ensure that the collected emission spectrum reflects only the average environment of the tryptophan residues, each beta-lactamase construct was excited at 295 nm and the emission spectrum from 300 nm to 450 nm was recorded. The wild-type beta-lactamase displayed an emission maximum at 347 nm, which is slightly blue-shifted compared to tryptophan in water (350 nm). All the mutant enzymes displayed the expected reduction in emission intensity due to the loss of a W229 in the sequence, but they also revealed both an additional blue-shift of the emission maximum compared to the wild-type, as well as a significant structuring of the spectra (Figure 1D). This finding indicates that at least one of the remaining tryptophan residues experienced a much more hydrophobic environment in the mutant enzymes. Based on the structural information available for TEM-1 the most likely reporter of this change in local environment would be W290.

Taken together, the SEC, CD and fluorescence data suggest that even though the mutant enzymes preserve their secondary structures, there are important local rearrangements impacting both the overall packing of the enzyme resulting in a more open and flexible global 3D structure in addition to altering the hydrophobicity around the allosteric site.

Point mutations in the PWP triad cause a 10-fold decrease in enzyme expression levels

Both the wild-type and the mutant enzymes were expressed and purified identically using *E. coli* BL21 (DE3) expression system followed by Ni^{2+} affinity chromatography (Figure 3). While the wild-type enzyme was expressed and purified efficiently

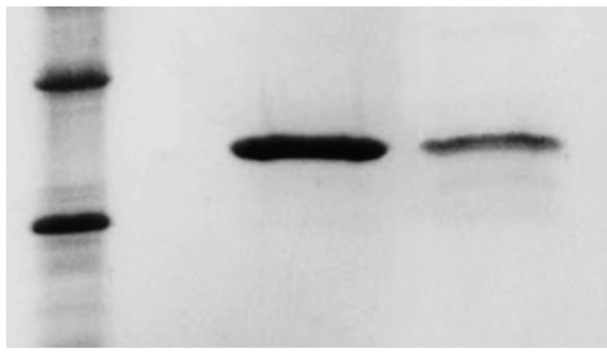

Figure 3. Electrophoretic analysis of TEM-1 beta-lactamase on denaturing gels. Protein standard (25 kDa and 35 kDa) (lane 1), wild-type (lane 2) and W229A (lane 3) beta-lactamases following purification with Ni^{2+}-affinity chromatography.

($\sim$0.89 mg L^{-1} culture), expression levels of the mutant enzymes were 10-fold lower ($\sim$0.08 mg L^{-1} culture). To rule out the possibility that beta-lactamase was partitioning to the cytoplasmic extracts during purification, the remaining pellets for the mutants were resuspended after the extraction of periplasmic proteins, in 5 mL 50 mM Tris buffer (pH 7.8) and sonicated on ice. Electrophoretic analysis showed that neither the cytoplasmic extracts nor the urea solubilized protein aggregates post extraction from cell pellet contained any detectable beta-lactamase.

One other explanation for the low yield for mutant enzymes could be that only a small fraction of the synthesized mutant beta-lactamase acquires a native-like conformation, while the remaining polypeptides fold into alternative conformations with decreased chemical stability, resulting in a faster clearance in the cell via intrinsic proteases.

The PWP triad is sequentially and structurally conserved in class a beta-lactamase family

The sequence conservation of the PWP triad was examined using the Consurf server[27,28]. In the Consurf scoring scheme, 0 represents no conservation and 9 represents 100% conservation. Of the 415 homologs of TEM-1 beta-lactamase (PDB ID: 1ZG4) identified using CS-Blast, all the members annotated in Uniprot (The UniProt Consortium 2015)[30], belonged to the class A beta-lactamases. The calculated individual conservation scores after alignment of these sequences were 9 for both P226 and W229 indicating that these residues of the PWP triad are absolutely conserved in class A beta-lactamases, similar to other functionally conserved regions such as the active site catalytic residues (S70, K73, S130, E166, K/R244) or the omega loop ligand binding residues (R164, E166) that also have ConSurf scores of 9 (Figure 4). P252 has a conservation score of 8 and it is conserved in 97.75% of the examined sequences.

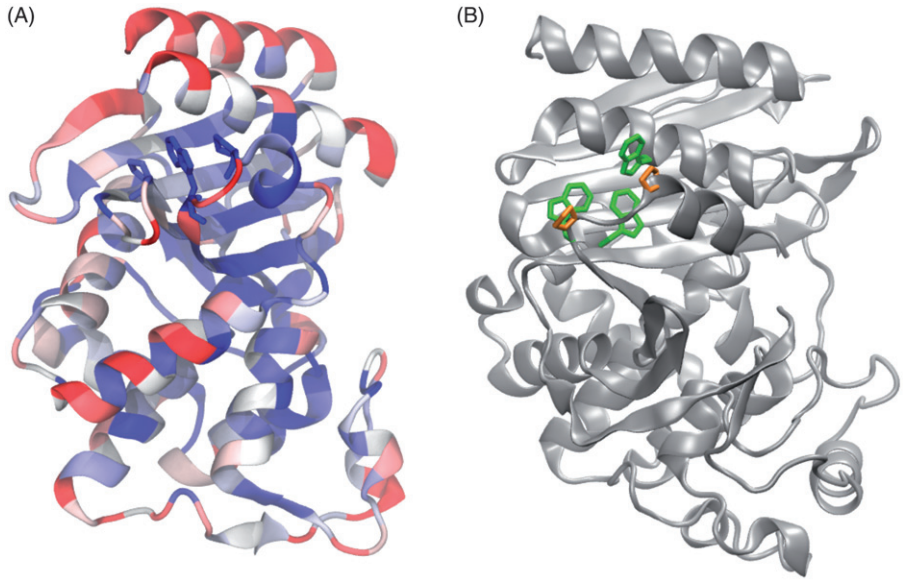

Figure 4. The PWP triad in class A beta-lactamase TEM-1 and the proline-tryptophan rich region in class C beta-lactamase AmpC; (A) TEM-1 beta-lactamase structure[14] colored according to conservation score as calculated by Consurf[27]. The backbone is shown with cartoon representation and P226, W229 and P252 side chains are shown as sticks. The most variable positions (ConSurf scores: 1–3) are colored red (light gray in print), intermediately conserved positions (ConSurf scores: 4–6) are white while the most conserved positions (ConSurf scores: 7–9) are colored blue (dark gray in print), (B) AmpC (class C, PDB ID: 1L2S) structure shown in cartoon representation with tryptophan and proline residues shown in stick representation. Tryptophan residues are in green and proline residues are in orange in the online version. The structure figures were created using VMD[55]. (The color figure can be found in the online version of the manuscript.)

To determine the prevalence for the structural conservation of the PWP stacking interaction in proteins, swisspdb[29] was used to search for the PWP motif in the 90% nonredundant set of 14 341 X-ray structures in the Protein Data Bank (PDB). When the search was conducted using the entire triad (P226–W229–P252), all of the nine proteins identified (Beta-lactamase from *Scaphirhynchus albus* 1BSG, Cephalosporinase 1HZO, BS3 1I2S, Toho-1 1IYS, TEM-1 1JTD, 1M40, SHV-2 1N9B, SHV-1 2G2U, CTX-M-9 2P74, Sed 3BFF) were class A beta-lactamases. When the search was repeated for paired selection of P226–W229 or W229–P252 only a small subset of the identified structures (13/339 and 9/31, respectively) belonged to the class A or class C beta-lactamases with the remaining structures representing a diverse set of scop folds. These results suggest that while proline–tryptophan or tryptophan–proline interaction is common in many different protein–protein or domain–domain interaction interfaces[31], the PWP triad formation identified in TEM-1 is unique to class A beta-lactamases.

Table 3 shows the list of representative beta-lactamase structures for which we examined the structural features around the PWP triad. The comparison of the two crystal structures of TEM-1 beta-lactamase with and without the allosteric inhibitor (1PZO and 1ZG4, respectively) shows a significant change in the orientation of the H10 helix and an accompanying decrease in the distances between the three residues of the PWP triad in the presence of the inhibitor, further indicating that the PWP triad and the hydrophobic groove along H10 communicate with each other.

We have previously shown by ligand based network analysis that class A and class C beta-lactamases bind to similar inhibitors[7], suggesting that the active site is structurally similar for ligand recognition. On the other hand, class A active site inhibitors such as clavulanic acid have lower effect on class C beta-lactamases[32]. Since the two classes have been reported to display similar ligand binding specificities to their active sites with varying affinities, we performed an additional sequence and structural analysis, this time focusing on the allosteric binding site, the PWP triad and its surrounding local environment. Our findings indicate that in class C beta-lactamase structures, represented by ampC beta-lactamase (Figure 4B)[33], both H10 and one of the prolines (corresponding to P252) are strictly conserved elements, but the PWP triad residues are sequentially rearranged to preserve the overall hydrophobic environment at the H10 N-terminus. Based on the sequence alignment of 15 selected class C beta-lactamases including AmpC, CMY-2, CMY-6, CMY-10 and FOX-7 as well as DHA-1, the W229 position of the class A PWP repeat is either conserved or replaced by Y or L, while replacements and rearrangements around the P226 position allow for direct hydrophobic contributions from neighboring W312, which can also be present as Y or L. Our findings show that while the PWP triad is unique to class A beta-lactamases, the properties and structural arrangement of corresponding residues in class C beta-lactamases create a similar hydrophobic environment to that of class A beta-lactamases. These results have important implication for drug design, as they clearly highlight the importance of the hydrophobic environment in allosteric ligand binding for these two classes of beta-lactamases.

On the other hand, class B beta-lactamases, also called metallo beta-lactamases represented by NDM-1 (PDB ID: 3ZR9)[34] have a completely different fold. Class D beta-lactamases, represented by the OXA family (PDB ID: 1K55)[35], lack the H10 helix and therefore these two classes are not expected to respond to allosteric inhibitors developed against the H10 helix site.

The PWP triad residues and their conformation are conserved even in the four resurrected precambrian beta-lactamases, GNCA[36], ENCA[36], PNCA[37] and ALL-CON[37]. Furthermore, MD simulations on both TEM-1 and precambrian beta-lactamases show that H10 and H11 helices and W229 display similar flexibility while P226 and P252 are rigid[17] suggesting the importance of the PWP triad dynamics in modulation of allostericity.

The contribution of CH-π hydrogen bonds and specifically proline–tryptophan interactions to protein–protein interactions and to protein stability has been recognized for over forty years[38–41]. In most of the domain–proline rich motif interactions, the proline residues and the hydrophobic residues are coplanar[31] and the tryptophan residues interact with proline via the tryptophan ''face'' rather than the ''edge''[42]. Moreover, in most CH-π H-bonds that involve tryptophan–proline interaction, the rings are aligned in an off-centered or displaced parallel stacking conformation[43]. These tryptophan–proline interactions established in the stacked and L-shaped configurations are very stable and can contribute to the stability of the folded state via intramolecular contacts as well as to intermolecular recognition[44]. The PWP triad geometry is also in an off-centered stacking interaction in class A and the precambrian beta-lactamases, suggesting that this stable and highly conserved

Table 3. Representative beta-lactamase structures examined.

Name	Class	PWP conservation	PDB code	Reference
TEM-1	A	Yes	1ZG4, 1BTL, 1M40, 1PZO	14,45,46,18
Toho-1	A	Yes	1IYS	47
CTX-M9a	A	Yes	2P74	48
SHV-1	A	Yes	1SHV, 2ZD8	21,49
NDM-1	B	Different fold	4EYB, 4RL0	50,51
AmpC	C	Prolines are conserved. Tryptophan is not conserved	1L2S, 1KE4, 2FFY	33,52,53
OXA-10	D	Helix10 missing	3LCE, 1K55	54,35
PNCA (3GA)	Precambrian	Yes	4C6Y	37
GCNA (2GA)	Precambrian	Yes	4B88	36
ENCA (1GA)	Precambrian	Yes	3ZDJ	36
ALL-CON	Precambrian	Yes	4C75	37

interaction is critical for the function and dynamics of beta-lactamases in the evolutionary process.

Conclusion

Beta-lactamases are ancient enzymes and as such their structure, evolution and catalytic mechanism have been examined in extensive detail but the discovery of an allosteric site formed by the outward rotation of H10 from the enzyme core in TEM-1 and SHV-1 has opened a new gate toward the design of novel inhibitors that target this hydrophobic binding site. In this work, we used computational and experimental analysis to focus on the PWP triad located at the N-terminus of the H10 helix to determine its significance for enzyme structure and activity. Our data shows that the PWP triad communicates with this allosteric site and regulates its structure, dynamics and stability. Point mutations within this triad result in significant or complete loss of enzyme activity as well as a more open and dynamic global structure with decreased chemical stability and increased aggregation propensity. The decrease in the overall solubility of the enzyme limited experimental studies to low working enzyme concentrations but the importance of size, but not polarity, was clearly established by detailed biophysical analysis of the W229Y and W229F mutants. The relative importance of the loss of aromaticity versus further reduction in size in almost a complete loss of activity for the W229A mutant remains as an answered question. Although the mutant enzymes preserve their secondary structures, local arrangements in the structure alter the overall packing of the enzyme resulting in a more open and flexible global 3D structure as well as decreased hydrophobicity around the allosteric site, which explains the significant loss in enzyme activity.

Both the sequence analysis of the triad using ConSurf server and the analysis of the existing crystal structures with swisspdb showed that while the pairwise proline-tryptophan or tryptophan–proline interactions were common in many different protein–protein or domain–domain interaction interfaces, the PWP triad is highly conserved and unique to class A beta-lactamases. The binding of the allosteric inhibitors to the groove formed between H10 and H11 suggests that H10 is a mobile element. Indeed, we showed that the dynamics of this region is critical for the communication with the active site[16]. Orthosteric inhibitors that recognize class A beta-lactamases[7] can also bind class C beta-lactamases[7], although with weaker affinity. On the other hand, conservation of the hydrophobic environment at the H10 N-terminus in both classes suggests that specific allosteric inhibitors directed for the H10 groove might be designed to recognize and inhibit not only class A beta-lactamases but also class C beta-lactamases and their specificity and selectivity might be optimized for each class with minor adjustments to the same core design. These computational analyses do not provide a direct mechanistic explanation of how the activity is modulated by the PWP triad, but its conservation at the sequence and structure level provide valuable clues about its evolutionary significance. Taken together, the findings of this work underscore the importance of the PWP triad in the regulation of enzyme activity in class A beta-lactamases through a unique interaction network at the recently identified allosteric site and highlight the potential for this signature region to become an effective inhibitor design target.

Acknowledgements

We thank Dr. Olga Gursky for providing Circular Dichroism and Fluorescence Spectroscopy facilities and for many helpful discussions.

Declaration of interest

The authors report no declarations of interest. This work was supported by TUBITAK Research Grants 113M533 (BSA) and 109M229 (EO), 114M179 (EO), Marmara University Research Foundation FEN-C-YLP-181208-0290 (BSA) and Boğaziçi University Research Foundation 14A05D7 (EO).

References

1. Wilke MS, Lovering AL, Strynadka NC. Beta-lactam antibiotic resistance: a current structural perspective. Curr Opin Microbiol 2005;8:525–33.
2. Fisher JF, Meroueh SO, Mobashery S. Bacterial resistance to beta-lactam antibiotics: compelling opportunism, compelling opportunity. Chem Rev 2005;105:395–424.
3. Perez F, Endimiani A, Hujer KM, Bonomo RA. The continuing challenge of ESBLs. Curr Opin Pharmacol 2007;7:459–69.
4. Pitout JD, Laupland KB. Extended-spectrum β-lactamase-producing Enterobacteriaceae: an emerging public-health concern. Lancet Infect Dis 2008;8:159–66.
5. Akyala AI, Alsam S. Extended spectrum beta-lactamase producing strains of *Salmonella* species – a systematic review. J Microbiol Res 2015;5:57–70.
6. Winkler ML, Bonomo RA. SHV-129: a gateway to global suppressors in the SHV β-lactamase family? Mol Biol Evol 2016;33:429–41.
7. Oztürk H, Ozkirimli E, Ozgur A. Classification of beta-lactamases and penicillin binding proteins using ligand-centric network models. PLoS One 2015;10:e0117874.
8. Budeyri-Gokgoz N, Yalaz S, Avcı NG, et al. Investigation of the in vivo interaction between β-lactamase and its inhibitor protein. Turk J Biol 2015;39:485–92.
9. Alaybeyoglu B, Sariyar-Akbulut B, Ozkirimli E. A novel chimeric peptide with antimicrobial activity. J Pept Sci 2015;21:294–301.
10. Ambler RP. The structure of beta-lactamases. Philos Trans R Soc Lond B Biol Sci 1980;289:321–31.
11. Bush K, Jacoby GA. Updated functional classification of beta-lactamases. Antimicrob Agents Chemother 2010;54:969–76.

12. Massova I, Mobashery S. Kinship and diversification of bacterial penicillin-binding proteins and beta-lactamases. Antimicrob Agents Chemother 1998;42:1–17.
13. Zhang Z, Palzkill T. Dissecting the protein–protein interface between beta-lactamase inhibitory protein and class A beta-lactamases. J Biol Chem 2004;279:42860–6.
14. Stec B, Holtz KM, Wojciechowski CL, Kantrowitz ER. Structure of the wild-type TEM-1 beta-lactamase at 1.55 A and the mutant enzyme Ser70Ala at 2.1 A suggest the mode of noncovalent catalysis for the mutant enzyme. Acta Crystallogr D Biol Crystallogr 2005; 61:1072–9.
15. Fisette O, Morin S, Savard PY, et al. TEM-1 backbone dynamics-insights from combined molecular dynamics and nuclear magnetic resonance. Biophys J 2010;98:637–45.
16. Meneksedag D, Dogan A, Kanlikilicer P, Ozkirimli E. Communication between the active site and the allosteric site in class A beta-lactamases. Comput Biol Chem 2013;43:1–10.
17. Zou T, Risso VA, Gavira JA, et al. Evolution of conformational dynamics determines the conversion of a promiscuous generalist into a specialist enzyme. Mol Biol Evol 2015;32:132–1.
18. Horn JR, Shoichet BK. Allosteric inhibition through core disruption. J Mol Biol 2004;336:1283–91.
19. Bowman GR, Geissler PL. Equilibrium fluctuations of a single folded protein reveal a multitude of potential cryptic allosteric sites. Proc Natl Acad Sci USA 2012;109:11681–6.
20. Reynolds KA, Thomson JM, Corbett KD, et al. Structural and computational characterization of the SHV-1 beta-lactamase-beta-lactamase inhibitor protein interface. J Biol Chem 2006;281: 26745–53.
21. Kuzin AP, Nukaga M, Nukaga Y, et al. Structure of the SHV-1 beta-lactamase. Biochemistry 1999;38:5720–7.
22. Seidman CE, Struhl K, Sheen J, Jessen T. Introduction of plasmid DNA into cells. Curr Protoc Mol Biol 2001;37:1.8:1.8.1–8.10.
23. Nossal NG, Heppel LA. The release of enzymes by osmotic shock from *Escherichia coli* in exponential phase. J Biol Chem 1966;241: 3055–62.
24. Bradford MM. A rapid and sensitive method for the quantitation of microgram quantities of protein utilizing the principle of protein–dye binding. Anal Biochem 1976;72:248–54.
25. Laemmli UK. Cleavage of structural proteins during the assembly of the head of bacteriophage T4. Nature 1970;227:680–5.
26. Blakesley RW, Boezi JA. A new staining technique for proteins in polyacrylamide gels using coomassie brilliant blue G250. Anal Biochem 1977;82:580–2.
27. Ashkenazy H, Erez E, Martz E, et al. ConSurf 2010: calculating evolutionary conservation in sequence and structure of proteins and nucleic acids. Nucleic Acids Res 2010;38:W529–33.
28. Celniker G, Nimrod G, Ashkenazy H, et al. ConSurf: using evolutionary data to raise testable hypotheses about protein function. Isr J Chem 2013;53:199–206.
29. Johansson MU, Zoete V, Michielin O, Guex N. Defining and searching for structural motifs using DeepView/Swiss-PdbViewer. BMC Bioinformatics 2012;13:173.
30. The UniProt Consortium. UniProt: a hub for protein information. Nucleic Acids Res 2015;43:D204–12.
31. Ball LJ, Kühne R, Schneider-Mergener J, Oschkinat H. Recognition of proline-rich motifs by protein–protein-interaction domains. Angew Chem Int Ed Engl 2005;44:2852–69.
32. Jacoby GA. AmpC beta-lactamases. Clin Microbiol Rev 2009;22: 161–82.
33. Powers RA, Morandi F, Shoichet BK. Structure-based discovery of a novel, noncovalent inhibitor of AmpC beta-lactamase. Structure 2002;10:1013–23.
34. Green VL, Verma A, Owens RJ, et al. Structure of New Delhi metallo-β-lactamase 1 (NDM-1). Acta Crystallogr F Struct Biol Cryst Commun 2011;67:1160–4.
35. Golemi D, Maveyraud L, Vakulenko S, et al. Critical involvement of a carbamylated lysine in catalytic function of class D beta-lactamases. Proc Natl Acad Sci USA 2001;98:14280–5.
36. Risso VA, Gavira JA, Mejia-Carmona DF, et al. Hyperstability and substrate promiscuity in laboratory resurrections of precambrian β-lactamases. J Am Chem Soc 2013;135:2899–902.
37. Risso VA, Gavira JA, Gaucher EA, Sanchez-Ruiz JM. Phenotypic comparisons of consensus variants versus laboratory resurrections of precambrian proteins. Proteins 2014;82:887–96.
38. Tamres M. Aromatic compounds as donor molecules in hydrogen bonding. J Am Chem Soc 1952;74:3375–8.
39. Bhattacharyya R, Chakrabarti P. Stereospecific interactions of proline residues in protein structures and complexes. J Mol Biol 2003;331:925–40.
40. Kumar M, Balaji PV. C-H. . .pi interactions in proteins: prevalence, pattern of occurrence, residue propensities, location, and contribution to protein stability. J Mol Model 2014;20:2136.
41. Nishio M, Umezawa Y, Fantini J, et al. CH-π hydrogen bonds in biological macromolecules. Phys Chem Chem Phys 2014;16: 12648–83.
42. Samanta U, Pal D, Chakrabarti P. Environment of tryptophan side chains in proteins. Proteins 2000;38:288–300.
43. McGaughey GB, Gagné M, Rappé AK. pi-stacking interactions. Alive and well in proteins. J Biol Chem 1998;273: 15458–63.
44. Biedermannova L, Riley KE, Berka K, et al. Another role of proline: stabilization interactions in proteins and protein complexes concerning proline and tryptophane. Phys Chem Chem Phys 2008;10: 6350–9.
45. Jelsch C, Mourey L, Masson JM, Samama JP. Crystal structure of *Escherichia coli* TEM1 beta-lactamase at 1.8 A resolution. Proteins 1993;16:364–83.
46. Minasov G, Wang X, Shoichet BK. An ultrahigh resolution structure of TEM-1 beta-lactamase suggests a role for Glu166 as the general base in acylation. J Am Chem Soc 2002;124: 5333–40.
47. Ibuka AS, Ishii Y, Galleni M, et al. Crystal structure of extended spectrum beta-lactamase Toho-1: insights into the molecular mechanism for catalytic reaction and substrate specificity expansion. Biochemistry 2003;42:10634–43.
48. Chen Y, Bonnet R, Shoichet BK. The acylation mechanism of CTX-M beta-lactamase at 0.88 A resolution. J Am Chem Soc 2007;129: 5378–80.
49. Nukaga M, Bethel CR, Thomson JM, et al. Inhibition of class A beta-lactamases by carbapenems: crystallographic observation of two conformations of meropenem in SHV-1. J Am Chem Soc 2008; 130:12656–62.
50. King DT, Worrall LJ, Gruninger R, Strynadka NC. New Delhi metallo-β-lactamase: structural insights into β-lactam recognition and inhibition. J Am Chem Soc 2012;134:11362–2365.
51. Feng H, Ding J, Zhu D, et al. Structural and mechanistic insights into NDM-1 catalyzed hydrolysis of cephalosporins. J Am Chem Soc 2014;136:14694–7.
52. Powers RA, Shoichet BK. Structure-based approach for binding site identification on AmpC beta-lactamase. J Med Chem 2002;45: 3222–34.
53. Chen Y, Minasov G, Roth TA, et al. The deacylation mechanism of AmpC beta-lactamase at ultrahigh resolution. J Am Chem Soc 2006; 128:2970–6.
54. Johnson JW, Gretes M, Goodfellow VJ, et al. Cyclobutanone analogues of beta-lactams revisited: insights into conformational requirements for inhibition of serine- and metallo-beta-lactamases. J Am Chem Soc 2010;132:2558–60.
55. Humphrey W, Dalke A, Schulten K. VMD: visual molecular dynamics. J Mol Graphics 1996;14:33–8.